Free Vibration Analysis of Laminated Beam by Polynomial, Trigonometric, Exponential and Zig-Zag Theories

Free Vibration Analysis of Laminated Beam by Polynomial, Trigonometric, Exponential and Zig-Zag Theories.

E. Carrera[a]*, M. Filippi[a]†, E. Zappino[a]‡
[a]Department of Mechanical and Aerospace Engineering, Politecnico di Torino,
Corso Duca degli Abruzzi 24, 10129 Torino, Italy.

Submitted to

Author for correspondence:
E. Carrera, Professor of Aerospace Structures and Aeroelasticity,
Department of Aeronautic and Space Engineering,
Politecnico di Torino,
Corso Duca degli Abruzzi 24,
10129 Torino, Italy,
tel: +39 011 090 6836,
fax: +39 011 090 6899,
e-mail: erasmo.carrera@polito.it

*Professor of Aerospace Structures and Aeroelasticity, e-mail: erasmo.carrera@polito.it
†Ph.D student, e-mail: matteo.filippi@polito.it
‡Ph.D student, e-mail: enrico.zappino@polito.it

Abstract

A number of refined beam theories are discussed in this paper to trace the free vibration response of laminated beams, including thin-walled boxes. These theories were developed by expanding the unknown displacement variables over the beam section axes using Taylor type expansions, trigonometric series, exponential, hyperbolic and zig-zag functions. The Finite Element method is used to derive governing equations in weak form. These equations are written using the Unified Formulation introduced by the first author, in terms of fundamental nuclei, whose forms do not depend on the expansions used. The natural frequencies are compared with results available in the literature or with those obtained by the finite element models related to commercial software. A number of analyses were conducted to compare various theories, including Euler-Bernoulli and Timoshenko models. The advantages/disadvantages of using the different theories are discussed for significant problems related to laminated beams as well as thin-walled boxes.

It is shown that refined kinematic theories are able to yield a very accurate evaluation of fundamental as well as higher mode frequencies in a way comparable to three-dimensional analysis, but it is obtained with a strong reduction of computational costs.

1 Introduction

Nowadays, composite and sandwich structures are used in a wide variety of applications which include automobiles, aircraft as well as biomedical devices. These materials present excellent properties such as high specific stiffness and strength, ease of formability, wide range of operating temperatures and many others. Nevertheless, the composite materials exhibit a complex behaviour, which is governed by a wider number of parameters than conventional materials and, for this reason, 2-D plate and shell or 3-D solid models are often used in order to understand their mechanical response. On the other hand, the computational cost of these kinds of models can become prohibitive, especially in those cases in which non-linear and failure analyses are required. The refined 1-D formulations represent good alternatives. As is well-known, both the classical beam theory [1] and the first-order shear deformation theory [2], [3] are based on strong assumptions. Indeed, the former neglects the transverse shear deformations, while the latter foresees a uniform shear distribution along the cross-section of a beam. These models yield very poor results when dealing with moderately deep and laminated structures or when the sections are thin-walled and open. In the light of these considerations, several attempts have been made to analyze composite beams and a brief and not exhaustive review is given here. The analyses performed by Reddy *et. al* used parabolic distribution of the transverse shear strains in order to fulfill the free boundary condition for shear stress on the top and bottom surfaces ([4], [5]). Some more refined models have been presented by Surana *et al.* [6] and Matsunaga [7], [8] where Lagrange's polynomials and power series of the depth coordinate (z) are used for describing accurately the shear transverse stress distribution of composite beams. Another important class of refined theories is based on the use of trigonometric functions. For instance, in [9] and [10] a refined sine model combined with Heaviside function for each layer was tested, whereas in [11] the same authors introduced Murakami's zig-zag function [12] so as to take into account the discontinuity of the first derivative of the displacements. Many other plate theories are known in which alternatives to sinusoidal function are used ([13], [14], [15]). With regard to free vibration analysis, a great amount of research is available in the literature. For instance, Subramanian [16] presented two different 1-D finite elements for laminated beams, in which the odd powers of the z-coordinate (until the 5th order) are used for expanding the axial displacement and the even powers for the transverse displacement (until the 4th order). The main advantages of these models are the inclusion of the effects of transverse shear strain and of normal strain and, furthermore, the fulfilment of the free transverse shear stress condition on the top and bottom surfaces of the beam. Marur *et al.* [17] proposed using Taylor's series expansion for axial displacement in order to describe the warping of cross-sections of sandwich and composite beams without the need of a shear correction factor. Interesting mixed formulations have been presented in [18] and [19], where continuity of transverse stress and displacement fields is enforced through thickness. In [19], the theory has been extended to the Finite Element (FE) method by invoking the transverse stress components as the nodal degrees of freedom by applying elasticity relations. It is worth mentioning some applications of the Dynamic Stiffness Method (DSM). In [20] the first order shear deformation theory is used to take into account the important shear effects of laminated beams and to improve the prediction of flexural frequencies. Banerjee [21] improved this kinematic model by introducing the effect of material coupling between the bending and torsional modes of deformation. In [22] and [23], Banerjee focused his

attention on sandwich structures by embedding in DSM framework suitable kinematic models. Moreover, the theory presented by Howson *et al.* in [24] combined the features of DSM with the advantages of the FE method by allowing to account for nodal masses, spring supports and non-classical boundary conditions. The growing interest in the investigation of characteristics of spinning structures has given considerable impulse to the development of many theories devoted to the dynamic analyses of composite shafts, turbine blades and propellers. For instance, Hodges *et al.* presented methods able to detect flexural, extensional and torsional mode shapes of laminated thin-walled rectangular and circular beams. About ten years later, Cortińez *et al.* [25] and Mira Mitra *et al.* [26] introduced theoretical models for beams with arbitrary cross-section with open or closed contour. Both theories take into account shear deformability. Even Vo *et al.* [27] developed a one-dimensional finite element for analysing the thin-walled beams by limiting their study to closed rectangular cross-section.

It is clear that many attempts have been made (see also the reviews in [28] and [29]) to develop a general reliable theory able to capture the complex nature of the composite materials. The present paper aims to introduce and compare a large variety of refined 1-D beam models by considering the free vibration problems of laminated, sandwich and composite thin-walled structures including closed box. Recently, these new kinematic theories have been assessed in [30], in which symmetric and anti-symmetric cross-ply beams were subjected to several load conditions. The results are quite encouraging both in terms of deflections and stress distributions. These theories derive from Carrera's Unified Formulation (CUF), that offers a procedure to obtain refined structural models. The procedure makes it possible to consider the order and the types of theories as free input parameters. CUF was first developed for plate and shell models ([31], [32], [33], [34]) and later was extended to the beam model [35]. So far, the refined displacement fields have been written adopting N–order Taylor type expansions (TE) [36] of the section coordinates or using N-order Lagrange polynomials (LE) [37] which were defined on a set of sampling points belonging to the section. For example, as far as the TE model is concerned, static and dynamic analyses have been carried out on unconventional cross-sections (hollow cylindrical reinforced structures, airfoil, bridge-like cross-sections etc.) in [38] [39] [40], [41], [42] and [43]. For a thorough and clear description of CUF see [35].

In the present work, displacement components are defined by using Taylor-type, trigonometric, exponential, hyperbolic and miscellaneous series. Laminated and sandwich structures as well as thin-walled box beams are considered. The results are reported in terms of natural frequencies and they are compared with those found in the literature or obtained by finite element models.

2 Theories Considered

A brief overview of the displacement models which have been implemented and compared in the present work is given in the following sections.

2.1 Classical Theories

Linear distribution of the displacement u_y and a constant distributions of u_x and u_z across the cross-section (see Fig.1) is assumed by classical beam theories. The displacement field above the beam cross-

section is:

$$\begin{array}{lll} u_x = & u_{0x}\,(y) & \\ u_y = & u_{0y}\,(y) \quad +\theta\,(y)\,x & +\phi\,(y)\,z \\ u_z = & u_{0z}\,(y) & \end{array} \tag{1}$$

where u_{0x}, u_{0y}, u_{0z} are the displacements along the three directions; θ and ϕ are the rotations around $z-$ and $x-$ axis, respectively. The Euler-Bernoulli theory [1] introduces a further assumption to neglect the transverse shear deformations ϵ_{xy} and ϵ_{yz}. The related displacement field becomes:

$$\begin{array}{lll} u_x = & u_{0x}\,(y) & \\ u_y = & u_{0y}\,(y) \quad -u_{x,y}\,(y)\,x & -u_{z,y}\,(y)\,z \\ u_z = & u_{0z}\,(y) & \end{array} \tag{2}$$

However, the shear stress play an important role in various beam problems. By including the shear deformations ϵ_{xy} and ϵ_{yz}, the Eq.(1) represents the kinematic field of the Timoshenko theory [3] which could also be written in the following form:

$$\begin{array}{lll} u_x = & u_{0x}\,(y) & \\ u_y = & u_{0y}\,(y) \quad +(\epsilon_{xy} - u_{x,y})\,x & +(\epsilon_{yz} - u_{z,y})\,z \\ u_z = & u_{0z}\,(y) & \end{array} \tag{3}$$

which is equivalent to Eq.(1) and the shear strains (ϵ_{xy}, ϵ_{yz}) and bending contributions ($u_{x,y}$, $u_{z,y}$) are separate.

Even though the Timoshenko model provides a constant distribution of shear deformation above the cross-section, it is not able to detect more complex deformations/stress state of the cross-section, such as the out- and in-plane deformations and the bending/torsion coupling.

2.2 Refined Theories

Many attempts have been made to improve classical beam models. For instance, the warping functions (see [44], [45]) were introduced to detect the cross-section deformation:

$$\begin{array}{lllll} u_x = & u_{0x}\,(y) & & & \\ u_y = & u_{0y}\,(y) \quad +f\,(x)\,(\epsilon^o_{xy}) & -u_{x,y}\,x & +f\,(z)\,(\epsilon^o_{yz}) & -u_{z,y}\,z \\ u_z = & u_{0z}\,(y) & & & \end{array} \tag{4}$$

where $f(x)$ and $f(z)$ are the warping functions and ϵ^o_{xy}, ϵ^o_{yz} are the transverse shear strains measured on the beam reference axis. So far, Eq.(4) neglect the in-plane axial strains ϵ_{xx} and ϵ_{zz}. Theories (2), (3) and (4) are all based on hypotheses, which may be too restrictive.

To circumvent the problem, other higher-order theories have been derived such as Matsunaga's model [7] in which the displacement components are expressed as follows:

$$\begin{array}{ll} u_x = & 0 \\ u_y = & z^n\,u_{y_n} \\ u_z = & z^n\,u_{z_n} \end{array} \tag{5}$$

where, according to the generalized Einstein notation, the subscripts and superscripts indicate summation. However, for a complete removal of the inconsistencies we should assume the displacement field as an arbitrary expansion of generic functions (at least theoretically). Hence, we can write the displacements as:

$$\mathbf{u} = F_\tau(x,z)\mathbf{u}_\tau(y), \qquad \tau = 1,2,....,M \tag{6}$$

where u_τ is the displacement vector and M stands for the number of terms of the expansion. Since both the number of terms and the functions F_τ could depend on the features of the problems, they need to be chosen properly. Unfortunately, the major drawback of this method is the large number of related governing equations. The Carrera's Unified Formulation (CUF) represents a possible avenue to tackle this problem. In fact, the CUF offers a systematic procedure to obtain every kind of displacement theory, as showed in [31, 32, 38, 40, 46]. This approach permits us to deal with any-order of beam theories without need of *ad hoc* implementations. In line with Washizu [47], in previous works, Eq.(6) has been employed by adopting a Taylor expansion that uses 2D polynomials $x^i z^j$ as base (i and j are positive integers). The capabilities of these functions have been assessed in the literature. For example, the second-order displacement field is:

$$\begin{aligned} u_x &= u_{x_1} + x\ u_{x_2} + z\ u_{x_3} + x^2\ u_{x_4} + xz\ u_{x_5} + z^2\ u_{x_6} \\ u_y &= u_{y_1} + x\ u_{y_2} + z\ u_{y_3} + x^2\ u_{y_4} + xz\ u_{y_5} + z^2\ u_{y_6} \\ u_z &= u_{z_1} + x\ u_{z_2} + z\ u_{z_3} + x^2\ u_{z_4} + xz\ u_{z_5} + z^2\ u_{z_6} \end{aligned} \tag{7}$$

while the third-order displacement field becomes:

$$\begin{aligned} u_x &= u_{x_1} + x\ u_{x_2} + z\ u_{x_3} + x^2\ u_{x_4} + xz\ u_{x_5} + z^2\ u_{x_6} + x^3\ u_{x_7} + x^2z\ u_{x_8} + xz^2\ u_{x_9} + z^3\ u_{x_{10}} \\ u_y &= u_{y_1} + x\ u_{y_2} + z\ u_{y_3} + x^2\ u_{y_4} + xz\ u_{y_5} + z^2\ u_{y_6} + x^3\ u_{y_7} + x^2z\ u_{y_8} + xz^2\ u_{y_9} + z^3\ u_{y_{10}} \\ u_z &= u_{z_1} + x\ u_{z_2} + z\ u_{z_3} + x^2\ u_{z_4} + xz\ u_{z_5} + z^2\ u_{z_6} + x^3\ u_{z_7} + x^2z\ u_{z_8} + xz^2\ u_{z_9} + z^3\ u_{z_{10}} \end{aligned} \tag{8}$$

Equations 7 and 8 show two examples of refined displacement models. The classical models can be considered as a particular case of these expansions. If we compare the refined models with the one reported in Eq. 1 it is clear that both have the constant terms, u_{x_1}, u_{y_1} and u_{z_1}. The coefficients of the linear terms in Eq. 1, $\theta(y)$ and $\phi(y)$, correspond to u_{y_2} and u_{y_3} in Eq. 7 and 8. The terms over the linear one represent the warping of the section, higher the number of terms, more flexible is the cross-section. A remarkable feature is that classical beam theories are obtainable as particular cases of Taylor expansions. It should be noted that classical theories require reduced material stiffness coefficients to contrast Poisson's locking. Unless otherwise specified, for classical and first-order models Poisson's locking is corrected according to Carrera and Giunta [35].

2.3 Advanced Theories based on Trigonometric and Exponential Expansions

Many attempts have been made in which the displacement fields have been obtained by using different functions. Since CUF makes it possible to deal with higher-order theories and it is invariant with respect to both any order N and any type of $F_\tau(x,z)$ function, it is simple to define new kinematic models (see [35]). For example, if we adopt a trigonometric series, the displacement components become:

$$
\begin{aligned}
u_x &= \sin\left(\frac{\pi x}{a}\right) u_{x_1} + \cos\left(\frac{\pi x}{a}\right) u_{x_2} + \sin\left(\frac{\pi z}{b}\right) u_{x_3} + \cos\left(\frac{\pi z}{b}\right) u_{x_4} + \sin\left(2\frac{\pi x}{a}\right) u_{x_5} + \dots \\
u_y &= \sin\left(\frac{\pi x}{a}\right) u_{y_1} + \sin\left(\frac{\pi x}{a}\right) u_{y_2} + \sin\left(\frac{\pi z}{b}\right) u_{y_3} + \cos\left(\frac{\pi z}{b}\right) u_{y_4} + \sin\left(2\frac{\pi x}{a}\right) u_{y_5} + \dots \\
u_z &= \sin\left(\frac{\pi x}{a}\right) u_{z_1} + \sin\left(\frac{\pi x}{a}\right) u_{z_2} + \sin\left(\frac{\pi z}{b}\right) u_{z_3} + \cos\left(\frac{\pi z}{b}\right) u_{z_4} + \sin\left(2\frac{\pi x}{a}\right) u_{z_5} + \dots
\end{aligned}
$$

or by choosing an exponential expansion:

$$
\begin{aligned}
u_x &= e^{\left(\frac{x}{a}\right)} u_{x_1} + e^{\left(\frac{z}{b}\right)} u_{x_2} + e^{\left(2\frac{x}{a}\right)} u_{x_3} + e^{\left(2\frac{z}{b}\right)} u_{x_4} + \dots \\
u_y &= e^{\left(\frac{x}{a}\right)} u_{y_1} + e^{\left(\frac{z}{b}\right)} u_{y_2} + e^{\left(2\frac{x}{a}\right)} u_{y_3} + e^{\left(2\frac{z}{b}\right)} u_{y_4} + \dots \\
u_z &= e^{\left(\frac{x}{a}\right)} u_{z_1} + e^{\left(\frac{z}{b}\right)} u_{z_2} + e^{\left(2\frac{x}{a}\right)} u_{z_3} + e^{\left(2\frac{z}{b}\right)} u_{z_4} + \dots
\end{aligned}
$$

where a, b are the main cross-section dimensions.

2.4 Advanced zig-zag Theories

Murakami [12] introduced his function in the first order shear deformation theory with the purpose of reproducing the zig-zag form for the displacements of laminated plates. Due to the intrinsic anisotropy of multilayered structures, the first derivative of the displacement variables in the $z-direction$ is discontinuous. The considered function is able to describe the aforementioned discontinuity (see Fig1). Since it is possible to use the zig-zag function in CUF framework, hereafter the theories which contain the term are identified with the exponent $(^{zz})$. For example, $TE2^{zz}$:

$$
\begin{aligned}
u_x &= u_{x_1} + x\ u_{x_2} + z\ u_{x_3} + x^2\ u_{x_4} + xz\ u_{x_5} + z^2\ u_{x_6} + (-1)^k \zeta_k u_{x_{7Z}} \\
u_y &= u_{y_1} + x\ u_{y_2} + z\ u_{y_3} + x^2\ u_{y_4} + xz\ u_{y_5} + z^2\ u_{y_6} + (-1)^k \zeta_k u_{y_{7Z}} \\
u_z &= u_{z_1} + x\ u_{z_2} + z\ u_{z_3} + x^2\ u_{z_4} + xz\ u_{z_5} + z^2\ u_{z_6} + (-1)^k \zeta_k u_{z_{7Z}}
\end{aligned}
$$

where $\zeta_k = 2z_k/h_k$ is a non-dimensional layer coordinate and h_k the thickness of the $k-layer$. The exponent k changes the sign of the zig-zag term in each layer.

2.5 Advanced Theories based on Miscellaneous Expansions

To further improve the kinematic model, we can combine the different functions by obtaining miscellaneous expansions. One expansion is given below:

$$
\begin{aligned}
u_x &= u_{x_1} + x\ u_{x_2} + z\ u_{x_3} + x^2\ u_{x_4} + xz\ u_{x_5} + z^2\ + e^{\left(1\frac{x}{a}\right)} u_{x_6}\ + e^{\left(1\frac{z}{b}\right)} u_{x_7} + \sin\left(3\frac{\pi x}{a}\right) u_{x_8} \\
u_y &= u_{y_1} + x\ u_{y_2} + z\ u_{y_3} + x^2\ u_{y_4} + xz\ u_{y_5} + z^2\ + e^{1\left(\frac{x}{a}\right)} u_{y_6}\ + e^{\left(1\frac{z}{b}\right)} u_{y_7} + \sin\left(3\frac{\pi x}{a}\right) u_{y_8} \\
u_z &= u_{z_1} + x\ u_{z_2} + z\ u_{z_3} + x^2\ u_{z_4} + xz\ u_{z_5} + z^2\ + e^{\left(1\frac{x}{a}\right)} u_{z_6}\ + e^{\left(1\frac{z}{b}\right)} u_{z_7} + \sin\left(3\frac{\pi x}{a}\right) u_{z_8}
\end{aligned}
$$

Further cases will be directly described in the numerical discussion.

3 The FE Formulation of Various Theories.

A classical Finite Element technique is adopted with the purpose of easily dealing with arbitrary shaped cross-sections. The generalized displacement vector is given by:

$$\mathbf{u}_\tau(y) = N_i(y)\mathbf{q}_{\tau i} \tag{9}$$

where N_i are the shape functions and $\mathbf{q}_{\tau i}$ is the nodal displacement vector:

$$\mathbf{q}_{\tau i} = \left\{ \begin{array}{ccc} q_{u_{x_{\tau i}}} & q_{u_{y_{\tau i}}} & q_{u_{z_{\tau i}}} \end{array} \right\}^T \tag{10}$$

For the sake of brevity, the shape functions are not listed here. They can be found in the literature, for instance in [35] (§5.2.2). In this paper elements with 4 nodes (B4) are formulated using the Lagrange formulation, therefore a cubic approximation along the y axis is adopted. The functions are defined in the natural coordinates and transpose in the real coordinate in according with the isoparametric formulation. The theory order of the beam model is related to the expansion on the cross-section and it is not correlated with the number of nodes per element along the y axis. In other words, these two parameters are totally free and not related to each other. The stiffness and mass matrices of the elements and the external loadings, which are consistent with the model, are obtained via the Principle of Virtual Displacements:

$$\delta L_{int} = \delta L_{ext} + \delta L_{ine} \tag{11}$$

where L_{int} and L_{ine} are the strain energy and the work of inertial loadings, respectively, whereas L_{ext} is the work of external loadings and δ stands for virtual variation. If the work of external loadings is null, Eq.11 becomes:

$$\delta L_{ine} - \delta L_{int} = \int_V (\delta \boldsymbol{u}^T \rho \ddot{\boldsymbol{u}}) dV - \int_V (\delta \boldsymbol{\epsilon}_p^T \boldsymbol{\sigma}_p + \delta \boldsymbol{\epsilon}_n^T \boldsymbol{\sigma}_n) dV = 0 \tag{12}$$

in which the vector $\ddot{\boldsymbol{u}}$ is the acceleration vector. The stress, $\boldsymbol{\sigma}$, and strain, $\boldsymbol{\epsilon}$, components are considered grouped as follows:

$$\begin{array}{ll} \boldsymbol{\sigma}_p = \left\{ \begin{array}{ccc} \sigma_{zz} & \sigma_{xx} & \sigma_{zx} \end{array} \right\}^T, & \boldsymbol{\epsilon}_p = \left\{ \begin{array}{ccc} \epsilon_{zz} & \epsilon_{xx} & \epsilon_{zx} \end{array} \right\}^T \\ \boldsymbol{\sigma}_n = \left\{ \begin{array}{ccc} \sigma_{zy} & \sigma_{xy} & \sigma_{yy} \end{array} \right\}^T, & \boldsymbol{\epsilon}_n = \left\{ \begin{array}{ccc} \epsilon_{zy} & \epsilon_{xy} & \epsilon_{yy} \end{array} \right\}^T \end{array} \tag{13}$$

The subscript "p" stands for terms lying on the cross-section, while "n" stands for terms lying on the other planes, which are orthogonal to the cross-section. The linear strain-displacement relations and the Hooke's law are, respectively:

$$\begin{array}{l} \boldsymbol{\epsilon}_p = \boldsymbol{D_p} \boldsymbol{u} \\ \boldsymbol{\epsilon}_n = (\boldsymbol{D_{ny}} + \boldsymbol{D_{np}}) \boldsymbol{u} \end{array} \tag{14}$$

$$\begin{array}{l} \boldsymbol{\sigma}_p = \boldsymbol{C}_{pp} \boldsymbol{\epsilon}_p + \boldsymbol{C}_{pn} \boldsymbol{\epsilon}_n \\ \boldsymbol{\sigma}_n = \boldsymbol{C}_{np} \boldsymbol{\epsilon}_p + \boldsymbol{C}_{nn} \boldsymbol{\epsilon}_n \end{array} \tag{15}$$

For an orthotropic material the matrices of the material coefficients are:

$$\boldsymbol{C}_{pp}^k = \left[\begin{array}{ccc} \tilde{C}_{11}^k & \tilde{C}_{12}^k & \tilde{C}_{16}^k \\ \tilde{C}_{12}^k & \tilde{C}_{22}^k & \tilde{C}_{26}^k \\ \tilde{C}_{16}^k & \tilde{C}_{26}^k & \tilde{C}_{66}^k \end{array} \right], \quad \boldsymbol{C}_{pn}^k = \boldsymbol{C}_{np}^{T\,k} = \left[\begin{array}{ccc} 0 & 0 & \tilde{C}_{13}^k \\ 0 & 0 & \tilde{C}_{23}^k \\ 0 & 0 & \tilde{C}_{36}^k \end{array} \right], \quad \boldsymbol{C}_{nn}^k = \left[\begin{array}{ccc} \tilde{C}_{55}^k & \tilde{C}_{45}^k & 0 \\ \tilde{C}_{45}^k & \tilde{C}_{44}^k & 0 \\ 0 & 0 & \tilde{C}_{33} \end{array} \right] \tag{16}$$

For the sake of brevity, the explicit forms of the coefficients of the matrices $\boldsymbol{C}$ are not included here, but they can be found in Tsai [48] or Reddy [49]. The apex k refers to the layer, so each layer can have a different material. The virtual variation of the strain energy is rewritten using Eq.s (6), (9), (14) and (15) in a compact format it becomes:

$$\delta L_{int} = \delta {q_{\tau i}}^T \boldsymbol{K}^{ij\tau s} q_{si} \tag{17}$$

where $\boldsymbol{K}^{ij\tau s}$ is the stiffness matrix in the form of the fundamental nucleus. In a compact notation, it can be written as:

$$\begin{aligned}
\boldsymbol{K}^{ij\,\tau\,s} \;=\; & I_l^{\,ij} \lhd \left(\boldsymbol{D}_{np}^T\, F_\tau\, \boldsymbol{I}\right)\Big[\tilde{\boldsymbol{C}}_{np}^k \left(\boldsymbol{D}_p\, F_s\, \boldsymbol{I}\right) \;+\; \tilde{\boldsymbol{C}}_{nn}^k \left(\boldsymbol{D}_{np}\, F_s\, \boldsymbol{I}\right)\Big] \;+ \\
& \left(\boldsymbol{D}_p^T\, F_\tau\, \boldsymbol{I}\right)\Big[\tilde{\boldsymbol{C}}_{pp}^k \left(\boldsymbol{D}_p\, F_s\, \boldsymbol{I}\right) \;+\; \tilde{\boldsymbol{C}}_{pn}^k \left(\boldsymbol{D}_{np}\, F_s\, \boldsymbol{I}\right)\Big] \rhd_\Omega \;+ \\
& I_l^{\,ij,_y} \lhd \Big[\left(\boldsymbol{D}_{np}^T\, F_\tau\, \boldsymbol{I}\right)\tilde{\boldsymbol{C}}_{nn}^k \;+\; \left(\boldsymbol{D}_p^T\, F_\tau\, \boldsymbol{I}\right)\tilde{\boldsymbol{C}}_{pn}^k\Big]\, F_s \rhd_\Omega \boldsymbol{I}_{\Omega\, y} \;+ \\
& I_l^{\,i,_y j}\, \boldsymbol{I}_{\Omega\, y} \lhd F_\tau \Big[\tilde{\boldsymbol{C}}_{np}^k \left(\boldsymbol{D}_p\, F_s\, \boldsymbol{I}\right) \;+\; \tilde{\boldsymbol{C}}_{nn}^k \left(\boldsymbol{D}_{np}\, F_s\, \boldsymbol{I}\right)\Big] \rhd_\Omega \;+ \\
& I_l^{\,i,_y j,_y}\, \boldsymbol{I}_{\Omega\, y} \lhd F_\tau\, \tilde{\boldsymbol{C}}_{nn}^k\, F_s \rhd_\Omega \boldsymbol{I}_{\Omega\, y}
\end{aligned} \tag{18}$$

where:

$$\boldsymbol{I}_{\Omega\, y} \;=\; \begin{bmatrix} 0 & 0 & 1 \\ 1 & 0 & 0 \\ 0 & 1 & 0 \end{bmatrix} \qquad\qquad \lhd \ldots \rhd_\Omega \;=\; \int_\Omega \ldots \, d\Omega \tag{19}$$

$$\left(I_l^{\,ij},\, I_l^{\,ij,_y},\, I_l^{\,i,_y j},\, I_l^{\,i,_y j,_y}\right) \;=\; \int_l \left(N_i\, N_j,\; N_i\, N_{j,_y},\; N_{i,_y}\, N_j,\; N_{i,_y}\, N_{j,_y}\right) dy \tag{20}$$

The apex k indicates the layer so that the material is considered not constant in the integral over the cross-section Ω. This allows to investigate composite structure and non-homogeneous sections (see Fig.2).

As it stated in Eq.12, the virtual work of inertial loads for a composite structure is:

$$\delta L_{ine} = \int_V (\delta \boldsymbol{u}^T \rho^k \ddot{\boldsymbol{u}}) dV \tag{21}$$

where ρ^k stands for the density of different materials which constitute the cross-section. Eq.(21) is rewritten using Eq.s (6) and (9):

$$\delta L_{ine} = \int_l \delta \boldsymbol{q}_{\tau i}^T \boldsymbol{N}_i \left[\int_\Omega \rho^k (F_\tau \boldsymbol{I})(F_s \boldsymbol{I})\, d\Omega\right] \boldsymbol{N}_j \ddot{\boldsymbol{q}}_{sj}\, dy \tag{22}$$

where $\ddot{\boldsymbol{q}}$ is the nodal acceleration vector. The last equation can be written in the following compact manner:

$$\delta L_{ine} = \int_l \delta \boldsymbol{q}_{\tau i}^T \boldsymbol{M}^{ij\tau s} \ddot{\boldsymbol{q}}_{sj}\, dy \tag{23}$$

where $\boldsymbol{M}^{ij\tau s}$ is the mass matrix in the form of fundamental nucleus. Its components are:

$$\begin{gathered}
{M_{xx}}^{ij\tau s} = {M_{yy}}^{ij\tau s} = {M_{zz}}^{ij\tau s} = I_l^{ij} \lhd (F_\tau \rho^k \boldsymbol{I} F_s) \rhd \\
{M_{xy}}^{ij\tau s} = {M_{xz}}^{ij\tau s} = {M_{yx}}^{ij\tau s} = {M_{yz}}^{ij\tau s} = {M_{zx}}^{ij\tau s} = {M_{zy}}^{ij\tau s} = 0
\end{gathered} \tag{24}$$

It should be noted that no assumptions on the approximation order have been made. It is therefore possible to obtain refined beam models without changing the formal expression of the nucleus components of the stiffness matrix,$\boldsymbol{K}$, and of the mass matrix, $\boldsymbol{M}$. This is the key-point of CUF which permits, with only nine FORTRAN statements, to implement any-order beam theories. The undamped dynamic problem can be written as it follows:

$$\boldsymbol{M}\ddot{q} + \boldsymbol{K}q = 0 \tag{25}$$

where $\boldsymbol{q}$ is the vector of the nodal unknowns. Introducing harmonic solutions, $\boldsymbol{q} = \boldsymbol{q}_0 e^{i\omega t}$, it is possible to compute the natural frequencies, ω_k by solving an eigenvalues problem:

$$\left(-\omega_k^2 \boldsymbol{M} + \boldsymbol{K}\right) \boldsymbol{q}_k = 0 \tag{26}$$

where $\boldsymbol{q}_k$ is the $k\text{-}th$ eigenvector.

4 Numerical Results and Discussion

4.1 Nomenclature used to denote various expansions

This section aims to assess the accuracy of the various theories discussed in Section2. The expansions considered are summarized in Tab.(1) in which acronyms are introduced. In order to understand their meaning, we may refer to the following short expressions:

- functions with single trigonometric factor:

$$sx = \sin\left(m\frac{\pi x}{a}\right) \qquad cx = \cos\left(m\frac{\pi x}{a}\right) \qquad sz = \sin\left(n\frac{\pi z}{b}\right) \qquad cz = \cos\left(n\frac{\pi z}{b}\right)$$
$$sd = \sin\left(mn\frac{\pi xz}{ab}\right) \qquad cd = \cos\left(mn\frac{\pi xz}{ab}\right)$$

- functions with two trigonometric factors:

$$cc = \cos\left(m\frac{\pi x}{a}\right)\cos\left(n\frac{\pi z}{b}\right) \qquad cs = \cos\left(m\frac{\pi x}{a}\right)\sin\left(n\frac{\pi z}{b}\right)$$
$$sc = \sin\left(m\frac{\pi x}{a}\right)\cos\left(n\frac{\pi z}{b}\right) \qquad ss = \sin\left(m\frac{\pi x}{a}\right)\sin\left(n\frac{\pi z}{b}\right)$$

- hyperbolic functions:

$$chx = \cosh\left(mx\right) \qquad shx = \sinh\left(mx\right) \qquad chz = \cosh\left(nz\right) \qquad shz = \sinh\left(nz\right)$$

- exponential functions:

$$expx = e^{(mx)} \qquad expz = e^{(nz)}$$

where l, m, n, p are the numbers of waves along the x and z-direction. For instance, the first component of the displacement vector related to $E6$ with 13 terms of Tab.(1) corresponds to the following expansion:

$$u_x = F_\tau u_{x\tau} \tag{27}$$

where, in addition to the constant term, the functions F_τ become:

$$\begin{aligned} F_\tau &= \cosh(mx) \qquad m = 2, 3, 4 \\ F_\tau &= \sinh(mx) \qquad m = 5, 6, 7 \\ F_\tau &= \cosh(mz) \qquad m = 8, 9, 10 \\ F_\tau &= \sinh(mz) \qquad m = 11, 12, 13 \end{aligned}$$

If Taylor's expansions have been added to displacement fields, their order has been specified by the subscript. In the case that a complete expansion is used, the subscript is *'higher order polynomial'-c*, while in contrast, if only some polynomials are employed, their orders are explicitly reported and divided by a comma. For the sake of clarity, in the following are presented the examples related to the two mentioned options for the first component of the displacement field 27:

- $E2_{2-c}$ with 14 terms:

$$\begin{aligned} u_x = cost\ u_{x_1} + \sin\left(\frac{\pi x}{a}\right) u_{x_2} + \cos\left(\frac{\pi x}{a}\right) u_{x_3} + \sin\left(\frac{\pi z}{b}\right) u_{x_4} + \cos\left(\frac{\pi z}{b}\right) u_{x_5} + \\ + \sin\left(2\frac{\pi x}{a}\right) u_{x_6} + \cos\left(2\frac{\pi x}{a}\right) u_{x_7} + \sin\left(2\frac{\pi z}{b}\right) u_{x_8} + \cos\left(2\frac{\pi z}{b}\right) u_{x_9} + \\ + x\ u_{x_{10}} + z\ u_{x_{11}} + x^2\ u_{x_{12}} + xz\ u_{x_{13}} + z^2\ u_{x_{14}} \end{aligned}$$

- $E2_{1,3}$ with 15 terms:

$$\begin{aligned} u_x = cost\ u_{x_1} + \sin\left(\frac{\pi x}{a}\right) u_{x_2} + \cos\left(\frac{\pi x}{a}\right) u_{x_3} + \sin\left(\frac{\pi z}{b}\right) u_{x_4} + \cos\left(\frac{\pi z}{b}\right) u_{x_5} + \\ + \sin\left(2\frac{\pi x}{a}\right) u_{x_6} + \cos\left(2\frac{\pi x}{a}\right) u_{x_7} + \sin\left(2\frac{\pi z}{b}\right) u_{x_8} + \cos\left(2\frac{\pi z}{b}\right) u_{x_9} + \\ + x\ u_{x_{10}} + z\ u_{x_{11}} + x^3\ u_{x_{12}} + x^2 z\ u_{x_{13}} + xz^2\ u_{x_{14}} + z^3\ u_{x_{15}} \end{aligned}$$

4.2 Convergence study

It is useful to provide a few results from a convergence study of the finite elements used. For this reason a cantilever beam is considered as shown in Fig.3. The material is aluminum alloy with the Young Modulus and the Poisson ratio equal to 73 GPa and 0.33, respectively. The cross section is square and the aspect-ratio, L/h, is assumed to be 100. The reference solutions are provided by the following formula from the Euler-Bernoulli theory:

$$u_z(y = L) = \frac{F_z L^3}{3EI}$$

Tab.2 gives the results obtained using a variety of expansions. It should be noted that a higher number of elements (n_e) enhances the flexibility of the structure and the convergency strictly depends on both the order and the type of approximations.

4.3 Symmetric and antisymmetric cross-ply laminated beams

In the first two examples, symmetric $(0^0/90^0/0^0)$ and antisymmetric $(0^0/90^0)$ cross-ply laminated beams are studied. The effect of the beam dimensions and lamination on the natural frequencies and modes as well as on the accuracy of the proposed theories is investigated. The simply supported beams are constituted by orthotropic material, whose properties are:

$$E_L/E_T = 25 \qquad G_{LT}/G_{TT} = 2.5 \qquad \nu_{LT} = \nu_{TT} = 0.25$$

where L refers to the fiber direction and T refers to the normal direction. All laminae are assumed to be of the same thickness. For convenience, the natural angular frequencies * are presented in dimensionless form:

$$\bar{\omega} = \frac{L^2}{b}\sqrt{\frac{\rho}{E_T}}\,\omega$$

where L is the length of the beam and b the width of cross-section. The results are compared with those found in [50] where Giunta *et al.* provided closed form solutions by using CUF. The higher-order displacement theories have been obtained by adopting Taylor-type expansions and the relative results have been assessed with three-dimensional FEM solutions, reported as FEM $3D_{24}$ and FEM $3D_{20}$. In Tabs.3 and 4, the dimensionless frequencies of the symmetric beams are shown, for length-to-thickness ratios equal to 10 and 5, respectively. The first two modal shapes are pure flexural modes, which occur in different planes. When the beam becomes thicker, these modes interchange their order of appearance and, only with higher order displacement models, does the "modal swapping" become detectable. For both cases, the use of zig-zag function substantially improves the accuracy of the results for the flexural modal shape in $yz-plane$, while, for the remaining mode of deformation, the more effective models are the Taylor-type expansions and E8. By contrast, the third mode involves a torsional deformation, whose natural frequency is computed with acceptable accuracy by adopting the theories with the xz term (in other words, Taylor-type expansions and E8). The last two modes are shown in Fig.4. The axial/shear deformation appears as fourth and fifth mode, respectively. By comparing the results it is found that the frequency values obtained with TE8 and E2 are close to the reference solutions for both values of length-to thickness ratios. As far as the last shear modes are concerned, the zig-zag function once again determines a significant improvement of the solutions, indeed, if we consider TE3 expansion for L/h equal to 10, the relative error decreases from 6% to 0.2%. An antisymmetric laminated beam with length-to-thickness ratio equal to 5 is considered. The dimensionless angular frequencies are shown in Tab.5. In the case in point, the five modal shapes are: flexural on $yz-plane$, flexural/torsional on $xy-plane$, torsional, axial/shear and shear on $xy-plane$, respectively. For sake of clarity, the latter two deformation modes are shown in Fig.4-c and 4-d. Classical models are not able to detect the torsional mode and the shear mode because of their hypotheses, hence, variable kinematic models are needed. As in the previous examples, the accuracy of the computation of frequencies is affected by the choice of the functions as well as by the kind of modal shapes. For instance, TE6 and E8 yield precise results for torsional and coupled

*The angular frequency is $\omega = 2\pi f$ (rad/sec) whereas f is the frequency (Hz).

modes (modes II and III), E2, E3 and E6 seem suitable for detecting the axial/shear mode (IV), whereas the zig-zag function is more effective for shear modes (modes IV and V).

4.4 Sandwich Beams

The sandwich beams considered in this paper consist of structural face sheets (f) bonded to a core (c), whose material properties are:

$$E_f = 68.9GPa \qquad E_c = 179.14MPa \qquad G_f = 26.5GPa \qquad G_c = 68.9MPa$$

$$\rho_f = 2687.3Kg/m^3, \qquad \rho_c = 119.69Kg/m^3$$

The first structure has a rectangular cross-section, in which the thicknesses of the face sheets and the core are $h_f = 0.40624$mm and $h_c = 6.3475$mm, respectively and the width is assumed to be $b = 25.4$mm. The length is $L = 1.2187$ m and both ends are clamped. The results of the present theories are compared with those found in [24] and [23] where the experimental values of Raville [51] have been quoted, and with those of a three-dimensional FEM solution (see Tab.6). The modal shapes considered are the first six flexural modes on $yz - plane$ and the first two torsional ones. For these latter, it is worthy to note that the expansions TE7 and E8 furnish the best results whereas, for the flexural modes, the use of zig-zag term shows significant improvement of the related solutions, especially for TE1 and TE2.
The subsequent analysis involves a clamped-clamped sandwich beam with a lower length-to-thickness ratio ($L/h = 5$). The cross-section is square and the ratio h_c/h_f is assumed to be equal to 8. The first eight dimensionless frequencies are compared with those of FEM solution, in which solid elements $HEX20$ of $MSC\ NASTRAN^{©}$ are used. The values are presented in the following dimensionless form:

$$\bar{\omega} = \frac{L^2}{b}\sqrt{\frac{\rho_f}{G_f}}\,\omega$$

In the light of the results in Tab.7, it is clear that only refined kinematic models are able to describe the dynamic behaviour of this kind of structure. First of all, the improvements introduced by the zig-zag term are more evident than in the previous example. For instance, considering the natural dimensionless frequency computed with TE7, the relative error decreases from 12% to 0.05%. Furthermore, it must be noted that the mode VIII is detected only by the miscellaneous expansions (in which the order of Taylor-type polynomials is at least 4) and by E9 expansions. These latter furnish appreciable results for all eight dimensionless frequencies with a low number of degrees of freedom. Figure 5 shows the last three modal shapes (VI, VII and VIII).

4.5 Thin-Walled Box Beam

While the geometrical features of the structure are fixed and shown in Fig.6, the lamination scheme has changed. Three different cases are analyzed $(0^0/0^0/0^0/0^0)$, $(0^0/90^0/90^0/0^0)$ and $(45^0/-45^0/-45^0/45^0)$. The material properties are:

$$E_L = 144GPa \qquad E_T = 9.65GPa \qquad G_{LT} = 4.14GPa \qquad G_{TT} = 3.45GPa$$

$$\nu_{LT} = \nu_{TT} = 0.3, \qquad \rho = 1389 Kg/m^3$$

The ratios L/h, h/b and b/t_e are assumed to be 6.667, 2 and 10, respectively. For comparison purposes, the frequencies (Hz) relating to the first ten modal shapes computed by shell FEM solutions are considered and reported in Tab.8. In these models, the finite element used is the $QUAD4$ of $MSC\ NASTRAN^{©}$. Despite the structure being very complex, the variable kinematic models are able to describe its dynamic behaviour quite accurately. Indeed, by enriching the displacement fields, the expansions used predict flexural, torsional, coupled and shell-like modes with increasing accuracy for all lamination schemes. It is worthy to note that the E9-4 expansion furnishes results that are very close to reference solution, limiting the relative errors under 15% also for shell-like modal shapes (some of these are shown in Fig.7).

5 Concluding Remarks

In this work, the one-dimensional finite elements based on various displacement fields have been employed to perform free vibration analyses of the laminated and sandwich beams. Various stacking sequences, the aspect-ratios and boundary conditions have been investigated. The implementation of the finite elements have been carried out in accordance with Carrera's Unified Formulation. A large variety of 1D models have been compared and, in the light of the results obtained, the following final remarks can be made:

- the use of refined 1D models is mandatory in order to get acceptable results especially when thick structures are treated;
- the zig-zag function significantly improves the solutions relating to flexural and shear modes when thick laminated and sandwich beams are studied;
- as far as thin-walled structure is concerned, the variable kinematic models are able to predict with excellent accuracy the shell-like frequencies for different lamination schemes.

Although the difficulty in establishing the best solution is evident, the possibility of using a large variety of one-dimensional theories to study structures which require two- or three-dimensional solutions seems to be a remarkable advantage of the proposed formulation. Naturally more accurate evaluations have to be made when considering different kinds of structures and other displacement fields. Future studies could address the dynamic behaviour of the open thin-walled cross-sections as well as fixed or rotating composite blades.

References

[1] L. Euler. *Theory of elasticity*. Lausanne and Geneva: Bousquet, 1744.

[2] S. P. Timoshenko and J. N. Goodier. *Theory of elasticity*. McGraw-Hill, 1970.

[3] S. P. Timoshenko. On the correction for shear of the differential equation for transverse vibration of prismatic bars. *Philosophical Magazine*, 41:744–746, 1921.

[4] J. N. Reddy. A simple higher-order theory for laminated composites. *Journal of Applied Mechanics*, 51:745–752, 1984.

[5] J.N Reddy A.A. Khdeir. An exact solution for the bending of thin and thick cross-ply laminated beams. *Composite Structures*, 37:195–203, 1997.

[6] K.S. Surana and S.H. Nguyen. Two-dimensional curved beam element with higher-order hierarchical transverse approximation for laminated composites. *Computer and Structures*, 36:499–511, 1990.

[7] H. Matsunaga. Interlaminar stress analysis of laminated composite beams according to global higher-order deformation theories. *Composite Structures*, 55:105–114, 2002.

[8] H. Matsunaga. Interlaminar stress analysis of laminated composite and sandwich circular arches subjected to thermal/mechanical loading. *Composite Structures*, 60:345–358, 2003.

[9] P. Vidal and O. Polit. A family of sinus finite elements for the analysis of rectangular laminated beams. *Composite Structures*, 84:56–72, 2008.

[10] P. Vidal and O. Polit. Assessment of the refined sinus model for the non-linear analysis of composite beams. *Composite Structures*, 87:370–381, 2009.

[11] P. Vidal and O. Polit. A sine finite element using a zig-zag function for the analysis of laminated composite beams. *Composites: Part B*, 42:1671–1682, 2011.

[12] H. Murakami. Laminated composite theory with improved in–plane responses. *Journal of Applied Mechanics*, 53:661–666, 1986.

[13] M. Karama, K.S. Afaq, and S. Mistou. Mechanical behaviour of laminated composite beam by the new multi–layered laminated composite structures model with transverse shear stress continuity. *International Journal of Solids and Structures*, 40:1525–1546, 2003.

[14] J.L. Mantari, A.S. Oktem, and C. Guedes Soares. A new higher order shear deformation theory for sandwich and composite laminated plates. *Composites: Part B*, 43:1489–1499, 2012.

[15] N. Grover, D.K. Maiti, and B.N Singh. A new inverse hyperbolic shear deformation theory for static and buckling analysis of laminated composite and sandwich plates. *Composite Structures*, 95:667–675, 2013.

[16] P. Subramanian. Dynamic analysis of laminated composite beams using higher order theories and finite elements. *Composite Structures*, 73:342–353, 2006.

[17] S.R. Marur and T. Kant. Free vibration analysis of fiber reinforced composite beams using higher order theories and finite element modelling. *Journal of Sound and Vibration*, 194:337–351, 1996.

[18] M. Kameswara Rao, Y.M. Desai, and M.R. Chistnis. Free vibrations of laminated beams using mixed theory. *Composite Structures*, 52:149–160, 2001.

[19] G.S. Ramtekkar, Y.M. Desai, and A.H. Shah. Natural vibrations of laminated composite beams by using mixed finite element modelling. *Journal of Sound and Vibration*, 257:635–651, 2002.

[20] M. Eisenberger, H. Abramovich, and O. Shulepov. Dynamic stiffness analysis of laminated beams using a first order shear deformation theory. *Composite Structures*, 31:265–271, 1995.

[21] J.R. Banerjee. Frequency equation and mode shape formulae for composite timoshenko beams. *Composite Structures*, 51:381–388, 2001.

[22] J.R. Banerjee, C.W. Cheung, R. Morishima, M. Perera, and J. Njuguna. Free vibration of sandwich beams using the dynamic stiffness method. *International Journal of Solids and Structures*, 44:7543–7563, 2007.

[23] J.R. Banerjee, C.W. Cheung, R. Morishima, M. Perera, and J. Njuguna. Free vibration of a three-layered sandwich beam using the dynamic stiffness method and experiment. *International Journal of Solids and Structures*, 44:7543–7563, 2007.

[24] WP Howson and A Zare. Exact dynamic stiffness matrix for flexural vibration of three-layered sandwich beams. *Journal of Sound and Vibration*, 282:753–767, 2005.

[25] V.H. Cortnez and M.T. Piovan. Vibration and buckling of composite thin-walled beams with shear deformability. *Journal of Sound and Vibration*, 258:701–723, 2002.

[26] Mira Mitra, S. Gopalakrishnan, and M. Seetharama Bhat. A new super convergent thin walled composite beam element for analysis of box beam structures. *International Journal of Solids and Structures*, 41:1491–1518, 2004.

[27] jaehong Lee Thuc P. Vo. Free vibration of thin-walled composite box beams. *Composites Structures*, 84:11–20, 2008.

[28] Rakesh K. Kapania and S. Raciti. Recent advanced in analysis of laminated beams and plates, part i: Shear effects and buckling. *AIAA Journal*, 27:923–934, 1989.

[29] Rameshchandra P. Shimpi and Yuwaraj M. Ghugal. A review of refined shear deformation theories of isotropic and anisotropic laminated plates. *Journal of Reinforced Plastics and Composites*, 21:775–813, 2002.

[30] E. Carrera, M. Filippi, and E. Zappino. Laminated beam analysis by polynomial, trigonometric, exponential and zig-zag theories. *European Journal of Mechanics - A/Solids*. Accepted Manuscript.

[31] E. Carrera. Theories and finite elements for multilayered, anisotropic, composite plates and shells. *Archives of Computational Methods in Engineering*, 9(2):87–140, 2002.

[32] E. Carrera. Theories and finite elements for multilayered plates and shells: a unified compact formulation with numerical assessment and benchmarking. *Archives of Computational Methods in Engineering*, 10(3):216–296, 2003.

[33] E. Carrera. Assessment of theories for free vibration analysis of homogeneous and multilayered plates. *Shock and Vibration*, 3–4:261–270, 2004.

[34] E. Carrera, P. Nali, and S. Brischetto. Variational statements and computational models for multifiled problems and multilayered structures. *Mechanics of Advanced Materials and Strctures*, 15:182–198, 2008.

[35] E. Carrera, G. Giunta, and M. Petrolo. *Beam Structures. Classical and Advanced Theories.* Wiley, 2011.

[36] E. Carrera and G. Giunta. Refined beam theories based on a unified formulation. *International Journal of Applied Mechanics*, 2:117–143, 2010.

[37] E. Carrera, M. Petrolo, C. Wenzel, G. Giunta, and S. Belouettar. Higher order beam finite elements with only displacement degrees of freedom. pages 1–11, Sept. 2009. XIX Congresso AIMETA, Ancona (IT).

[38] E. Carrera, G. Giunta, P. Nali, and M. Petrolo. Refined beam elements with arbitrary cross-section geometries. *Computers and Structures*, 88(5–6):283–293, 2010. DOI: 10.1016/j.compstruc.2009.11.002.

[39] E. Carrera, M. Petrolo, and E. Zappino. Performance of cuf approach to analyze the structural behavior of slender bodies. *Journal of Structural Engineering*, 138:285–298, 2012.

[40] E. Carrera, M. Petrolo, and P. Nali. Unified formulation applied to free vibrations finite element analysis of beams with arbitrary section. *Shock and Vibrations*, 18(3):485–502, 2011. doi: 10.3233/SAV-2010-0528.

[41] M. Petrolo, E. Zappino, and E. Carrera. Refined free vibration analysis of one-dimensional structures with compact and bridge-like cross-sections. *Thin–Walled Structures*, 56:49–61, 2012. DOI: 10.1016/j.tws.2012.03.011.

[42] E. Carrera, M. Petrolo, and A. Varello. Advanced beam formulations for free vibration analysis of conventional and joined wings. *Journal of Aerospace Engineering*, 25(2):282–293, 2012. DOI: 10.1061/(ASCE)AS.1943-5525.0000130.

[43] E. Carrera, E. Zappino, and M. Filippi. Free vibration analysis of thin–walled cylinders reinforced with longitudinal and transversal stiffeners. *Journal of Vibration and Acoustics*, 135(1), 2013. doi: 10.1115/1.4007559.

[44] V. V. Novozhilov. *Theory of elasticity*. Pergamon, 1961.

[45] L. Dufort, S. Drapier, and M. Grdiac. Closed–form solution for the cross–section warping in short beams under three–point bending. *Composite Structures*, 52:233–246, 2011.

[46] E. Carrera and M. Petrolo. On the effectiveness of higher-order terms in refined beam theories. *Journal of Applied Mechanics*, 78(3), 2011. doi: 10.1115/1.4002207.

[47] K. Washizu. *Variational methods in elsticity and plasticity*. Pergamon Press, 1975.

[48] S. W. Tsai. *Composites Design*. Dayton, Think Composites, 4th edition, 1988.

[49] J. N. Reddy. *Mechanics of laminated composite plates and shells. Theory and Analysis*. CRC Press, 2^{nd} edition, 2004.

[50] G. Giunta, F. Biscani, S. Belouettar, A.J.M. Ferreira, and E. Carrera. Free vibration analysis of composite beams via refined theories. *Composites: Part B*, B 44:540–552, 2013. DOI: 10.1016/j.compositesb.2012.03.005.

[51] M.E. Raville, En-Sinh Ueng, and Ming-Min Lei. Natural frequencies of vibration of fixed-fixed sandwich beams. *Journal of Applied Mechanics*, 83:367–371, 1961.

	1	2	3	4	5	6	7	8	$\bar{9}$
$cost$	✓	✓	✓	✓	✓	✓	✓	✓	✓
sx	✓	✓	✓		✓		✓	✓	
cx		✓	✓						
sz	✓	✓	✓		✓		✓	✓	
cz		✓	✓						
sd			✓						
cd			✓						
$expx$				✓	✓				
$expz$				✓	✓				
shx						✓	✓		
chx						✓	✓		
shz						✓	✓		
chz						✓	✓		
$coxz$									✓
$csxz$									✓
$scxz$									✓
$sixz$									✓
xz								✓	
TE	✓	✓	✓	✓	✓	✓	✓		

$\bar{\bullet}$:$m \neq n$.

Table 1: Expansions.

	$n_e = 1$	$n_e = 5$	$n_e = 10$	$n_e = 30$
EBBT	1.3703	1.3703	1.3703	1.3703
FSDT	1.3704	1.3704	1.3704	1.3704
TE_1	1.3704	1.3704	1.3704	1.3704
TE_3	1.2728	1.3442	1.3534	1.3597
TE_5	1.2840	1.3541	1.3627	1.3684
Ref.eq.(4.2)=1.3698				

EBBT stands for Classical beam theory.

FSDT stands for First-order beam theory.

Table 2: Effect of the number (n_e) of elements B4 on $-u_z$ ($\times 10^{-3}$ $[m]$). Loading case: bending.

	Mode I	Mode II	Mode III	Mode IV	Mode V	DOFs
FEM $3D_{24}$[50]	10.035	10.334	17.642	126.60	218.28	5475
TE_{23} [50]	10.038	10.371	17.719	126.70	219.02	900
EBBT	11.697	13.929	-	129.52	-	198
FSDT	10.358	11.418	-	129.58	268.47	198
TE_2	10.367	11.420	20.968	128.46	268.50	396
	(10.367)	(10.450)	(20.968)	(128.75)	(221.10)	462
TE_3	10.113	10.637	20.968	128.78	233.05	660
	(10.113)	(10.337)	(20.968)	(128.74)	(218.85)	726
TE_6	10.069	10.501	18.005	127.24	224.88	1848
	(10.069)	(10.333)	(18.005)	(127.22)	(218.67)	1914
E1-5	10.176	10.426	21.075	129.61	220.32	726
	(10.176)	(10.351)	(21.075)	(129.61)	(218.91)	792
E2-4	10.174	10.416	21.088	127.86	220.24	1122
	(10.174)	(10.342)	(21.088)	(126.91)	(218.66)	1188
E3-3	10.173	10.416	21.032	128.18	220.23	1254
	(10.173)	(10.340)	(21.031)	(127.20)	(218.66)	1320
E5-2	10.188	10.491	21.475	128.07	258.00	594
	(10.188)	(10.350)	(21.471)	(128.61)	(218.95)	660
E6-2	10.173	10.656	21.075	127.99	233.73	594
	(10.173)	(10.342)	(21.075)	(125.78)	(218.94)	660
E7-2	10.173	10.428	21.075	126.18	258.00	858
E8-5	10.073	10.417	18.242	129.60	220.10	1386
	(10.073)	(10.342)	(18.241)	(129.22)	(218.68)	1452

(−): expansions with zig-zag term.

Table 3: Dimensionless natural frequencies, L/b=10, [0/90/0] beam.

	Mode I	Mode II	Mode III	Mode IV	Mode V
FEM $3D_{24}$[50]	6.8888	7.4968	9.0386	55.536	57.912
TE_{23} [50]	6.9252	7.5017	9.0683	55.914	58.135
EBBT	13.752	11.552	-	-	64.722
FSDT	8.0853	8.0409	-	-	64.752
TE_2	8.0837	8.0451	10.502	67.238	62.857
	(7.0131)	(8.0451)	(10.502)	(66.319)	(62.893)
TE_3	7.1597	7.6230	10.502	59.912	62.824
	(6.8990)	(7.6230)	(10.502)	(56.467)	(62.540)
TE_8	6.9800	7.5279	9.1129	56.694	58.670
	(6.8886)	(7.5279)	(9.1129)	(55.729)	(58.886)
E1-5	6.9675	7.6956	10.536	58.245	64.591
	(6.8943)	(7.6956)	(10.535)	(57.322)	(64.552)
E2-4	6.9653	7.6952	10.537	58.389	59.600
	(6.8913)	(7.6952)	(10.537)	(57.323)	(58.670)
E5-2	7.0480	7.7013	10.586	58.608	62.850
	(6.8969)	(7.7013)	(10.585)	(57.361)	(62.621)
E6-2	7.1752	7.6954	10.536	60.916	64.457
	(6.8973)	(7.6954)	(10.535)	(57.425)	(64.789)
E8-5	6.9649	7.5601	9.2726	56.174	63.833
	(6.8918)	(7.5601)	(9.2726)	(56.036)	(63.955)

(−): expansions with zig-zag term.

Table 4: Dimensionless natural frequencies, L/b=5, [0/90/0] beam.

	Mode I	Mode II	Mode III	Mode IV	Mode V	DOFs
FEM $3D_{20}$[50]	4.9357	6.4491	9.0672	33.566	50.448	3843
TE_{23} [50]	4.9375	6.4603	9.0852	33.718	50.640	900
EBBT	6.0083	10.102	-	57.186	-	198
FSDT	5.0738	7.5051	-	40.961	-	198
TE_2	5.0551	6.9637	10.133	37.566	63.570	396
	(5.0440)	(6.9632)	(10.133)	(36.384)	(59.734)	462
TE_3	4.9947	6.6601	9.8334	36.165	56.963	660
	(4.9942)	(6.6593)	(9.8330)	(33.851)	(53.001)	726
TE_6	4.9462	6.5042	9.1550	34.153	51.527	1848
	(4.9384)	(6.5037)	(9.1550)	(33.583)	(50.799)	1914
E1-6	5.0212	7.2227	10.235	37.565	60.877	858
	(4.9675)	(7.2227)	(10.235)	(34.202)	(55.170)	924
E1-4_{4-c}	4.9406	6.5510	9.2579	34.519	52.504	1518
	(4.9360)	(6.5503)	(9.2582)	(33.564)	(51.480)	1584
E2-4	4.9438	7.2222	10.237	33.957	54.648	1122
	(4.9381)	(7.2222)	(10.237)	(33.575)	(54.094)	1188
E2-3_{3-c}	4.9407	6.6589	9.8328	33.927	53.147	1452
	(4.9362)	(6.6586)	(9.8328)	(33.590)	(52.615)	1518
E3-4	4.9435	7.2154	10.237	33.920	54.637	1650
	(4.9381)	(7.2154)	(10.237)	(33.586)	(54.087)	1716
E4-4	5.0065	7.2356	10.238	34.749	57.884	594
	(5.0059)	(7.2356)	(10.236)	(33.775)	(54.525)	660
E5-3	4.9458	7.2220	10.235	34.525	55.559	858
	(4.9407)	(7.2220)	(10.235)	(33.613)	(54.139)	924
E6-2	(4.9518)	(7.2222)	(10.235)	(33.758)	(54.156)	660
E6-1_{3-c}	(4.9411)	(6.6586)	(9.8328)	(33.713)	(52.624)	990
E8-5	5.0014	6.5143	9.1995	37.205	57.391	1386
	(4.9650)	(6.5135)	(9.1975)	(34.175)	(51.864)	1452

(−): expansions with zig-zag term.

Table 5: Dimensionless natural frequencies, L/b=5, [0/90] beam.

	Mode I	Mode II	Mode III	Mode IV	Mode V	Mode VI	Mode VII	Mode VIII[a]	Mode IX[a]
Exper.[51]	-	-	185.50	280.30	399.40	535.20	680.70	-	-
[24]	34.597	93.100	177.16	282.78	406.33	544.33	693.79	-	-
DSM [23]	34.342	91.385	171.69	270.36	383.27	506.88	638.39	-	-
FEM 3D	34.817	93.676	178.20	284.37	408.44	546.93	696.77	298.97	598.88
EBBT	35.435	97.668	191.44	316.41	472.62	660.22	879.53	-	-
FSDT	35.418	97.563	191.09	315.53	470.77	656.75	873.58	-	-
TE_1	35.418	97.563	191.09	315.53	470.77	656.75	873.58	1137.9	2276.4
	(34.696)	(93.340)	(177.58)	(283.34)	(407.15)	(545.29)	(695.54)	(1137.9)	(2276.2)
TE_2	35.628	98.146	192.24	317.45	473.70	660.93	879.34	868.71	1738.2
	(34.895)	(93.853)	(178.50)	(284.72)	(408.97)	(547.56)	(698.15)	(867.86)	(1733.9)
TE_4	35.229	95.567	183.61	296.26	430.67	583.69	753.05	365.31	729.38
	(34.958)	(94.016)	(178.79)	(285.15)	(409.54)	(548.28)	(698.98)	(365.10)	(728.80)
TE_7	35.043	94.518	180.35	288.72	416.26	559.41	715.75	338.73	674.84
	(34.951)	(93.977)	(178.75)	(285.08)	(409.43)	(548.10)	(698.71)	(338.66)	(674.66)
E2-5	36.580	98.428	187.31	298.96	429.71	575.72	734.49	1139.0	2276.7
	(36.480)	(97.893)	(185.70)	(295.37)	(423.06)	(564.85)	(718.28)	(1139.0)	(2276.7)
E4-3_{3-c}	35.071	94.825	181.53	291.72	422.05	569.17	731.09	867.43	1733.4
	(34.982)	(93.836)	(178.28)	(284.84)	(409.31)	(547.13)	(701.35)	(867.23)	(1732.1)
E5-2_{2-c}	34.984	94.369	180.10	288.38	415.81	558.89	715.30	867.36	1733.2
	(34.892)	(93.845)	(178.48)	(284.69)	(408.92)	(547.50)	(698.05)	(867.26)	(1732.6)
E8-5	35.904	96.692	184.19	294.30	423.49	568.03	725.46	369.69	730.74
	(35.809)	(96.184)	(182.65)	(290.86)	(417.11)	(557.55)	(709.79)	(369.55)	(730.50)

(−): expansions with zig-zag term.

[a]: torsional mode.

Table 6: Comparative results for the natural frequencies [Hz] of a fixed-fixed sandwich beam.

	Mode I^a	Mode II^a	Mode III^c	Mode IV^a	Mode V^b	Mode VI*	Mode VII*	Mode VIII*	DOFs
FEM 3D	2.0308	4.3874	6.6198	7.3156	7.7618	10.461	10.603	10.673	68277
EBBT	14.373	35.786	-	61.872	9.4430	-	-	-	279
FSDT	10.367	22.116	-	35.737	7.9752	-	-	-	279
TE_1	10.368	22.116	15.118	35.737	7.9752	30.233	88.065	-	279
	(2.1069)	(4.6382)	(15.091)	(7.8576)	(8.8191)	(29.965)	(19.171)	-	372
TE_3	3.4838	7.1907	13.763	11.428	7.9197	31.614	21.320	-	930
	(2.1030)	(4.6302)	(15.896)	(7.8498)	(7.9198)	(29.963)	(11.445)	-	1023
TE_6	2.2745	4.8532	7.0430	7.9833	7.8136	12.188	12.294	12.252	2604
	(2.0325)	(4.3951)	(6.9046)	(7.3309)	(7.8136)	(11.402)	(11.032)	(12.252)	2697
TE_7	2.2687	4.8424	6.9949	7.9683	7.8120	11.847	11.971	12.234	3348
	(2.0319)	(4.3923)	(6.8579)	(7.3222)	(7.8120)	(11.162)	(10.805)	(12.234)	3441
E1-3_{4-c}	2.1753	4.6773	7.7521	7.4934	7.8533	13.142	12.132	19.943	1953
	(2.0386)	(4.4155)	(7.4239)	(7.3746)	(7.8533)	(12.710)	(11.330)	(19.943)	2046
E5-3	(2.0434)	(4.4312)	(15.079)	(7.4039)	(8.1020)	(29.911)	(11.378)	-	1302
E8-5	(2.1022)	(4.6233)	(7.3860)	(7.8253)	(7.8947)	(12.540)	(17.664)	-	2046
E9-2	(2.0343)	(4.3993)	(8.6952)	(7.3368)	(8.0206)	(12.493)	(13.502)	(16.390)	2418
E9-3	(2.0317)	(4.3914)	(6.9315)	(7.3220)	(7.8181)	(11.114)	(10.823)	(12.284)	4650
E9-4	(2.0299)	(4.3850)	(6.7931)	(7.3065)	(7.8055)	(10.924)	(10.760)	(11.698)	7626

$(-)$: expansions with zig-zag term.

$-$: results not provided by the model.

*: mode in Fig.5.

^{a}: bending mode in $z-direction$.

^{b}: bending mode in $x-direction$.

^{c}: torsional mode.

Table 7: Comparative results for the dimensionless frequencies of a fixed-fixed sandwich beam with $L/b = 5$.

	Mode I	Mode II	Mode III	Mode IV	Mode V	Mode VI	Mode VII	Mode VIII	Mode IX	Mode X
					0/0/0/0					
Shell	35.447[a]	58.533[b]	76.011[c]	114.23[a]	130.12[d]	143.15[d]	148.53[d]	163.65[d]	165.24[d]	170.34[a/d]
TE_4	38.345	60.171	89.811	144.93	851.27	1211.7	1215.8	1234.5	-	292.80
TE_7	36.849	59.290	85.739	134.58	223.95	177.53	191.41	220.26	203.65	259.63
TE_{11}	36.413	59.043	81.861	126.82	158.22	156.38	164.12	183.16	179.62	214.26
E9-3	36.531	59.330	85.285	126.86	168.24	161.12	167.96	185.29	185.68	212.43
E9-4	36.245	59.023	80.884	123.38	149.99	153.60	159.94	176.56	174.97	198.25
					0/90/90/0					
Shell	29.129[a]	48.813[b]	81.335[c]	112.37[a]	179.21[d]	182.70[b]	197.83[d]	205.38[a/d]	232.92[d]	235.97[d]
TE_4	30.677	49.286	88.939	129.58	909.06	191.71	890.10	273.58	2005.6	2023.8
TE_7	29.864	48.817	86.216	121.66	224.57	186.83	289.38	249.26	274.84	282.87
TE_{11}	29.656	48.676	84.545	118.26	199.82	185.45	231.79	229.71	249.48	254.09
E9-3	29.779	48.896	88.443	118.55	205.90	186.47	244.70	228.90	255.04	259.12
E9-4	29.588	48.669	84.245	116.93	194.16	185.27	220.72	221.75	245.46	249.23
					45/-45/-45/45					
Shell	15.803[a]	26.041[b]	96.012[a]	153.84[b]	168.38[d]	197.92[d]	209.19[e]	237.73[a/d]	267.17[d]	272.02[d]
TE_4	16.589	27.864	102.29	164.32	249.35	633.34	220.56	280.37	758.58	-
TE_7	16.161	26.901	98.862	158.69	213.82	286.75	212.40	261.79	353.18	334.85
TE_{11}	16.013	26.494	97.573	156.29	191.63	232.96	210.96	253.79	304.22	301.42
E9-3	16.813	27.552	98.811	158.27	197.68	240.00	211.83	257.77	311.19	306.99
E9-4	16.042	26.519	97.491	156.27	186.55	223.93	211.16	250.02	293.60	295.55

[a]: bending mode in $x-direction$.

[b]: bending mode in $z-direction$.

[c]: torsional mode.

[d]: shell-like mode.

[e]: axial mode.

Table 8: First ten frequencies (Hz) of rectangular thin-walled cantilever beams.

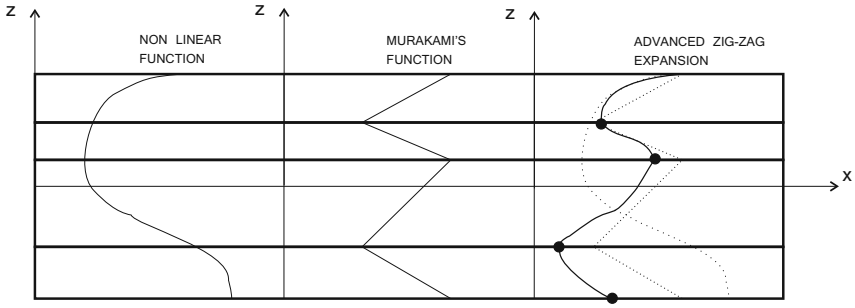

Figure 1: Inclusion of the Murakamis function to higher order distribution.

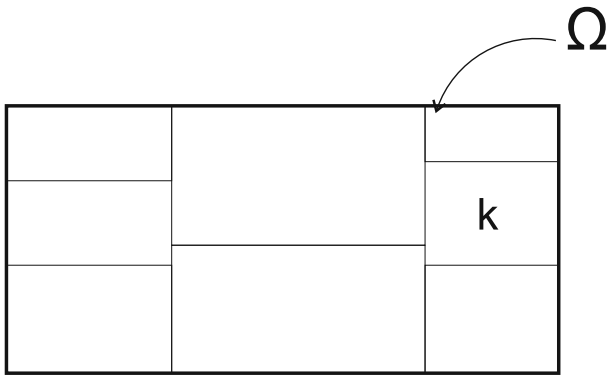

Figure 2: Sketch of a generic non-homogeneous cross-section Ω.

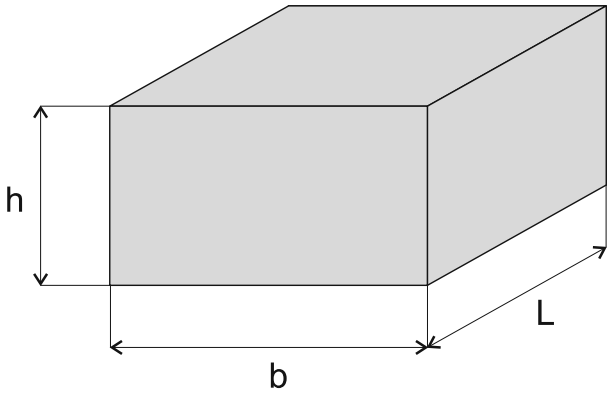

Figure 3: Sketch of beam and its dimensions.

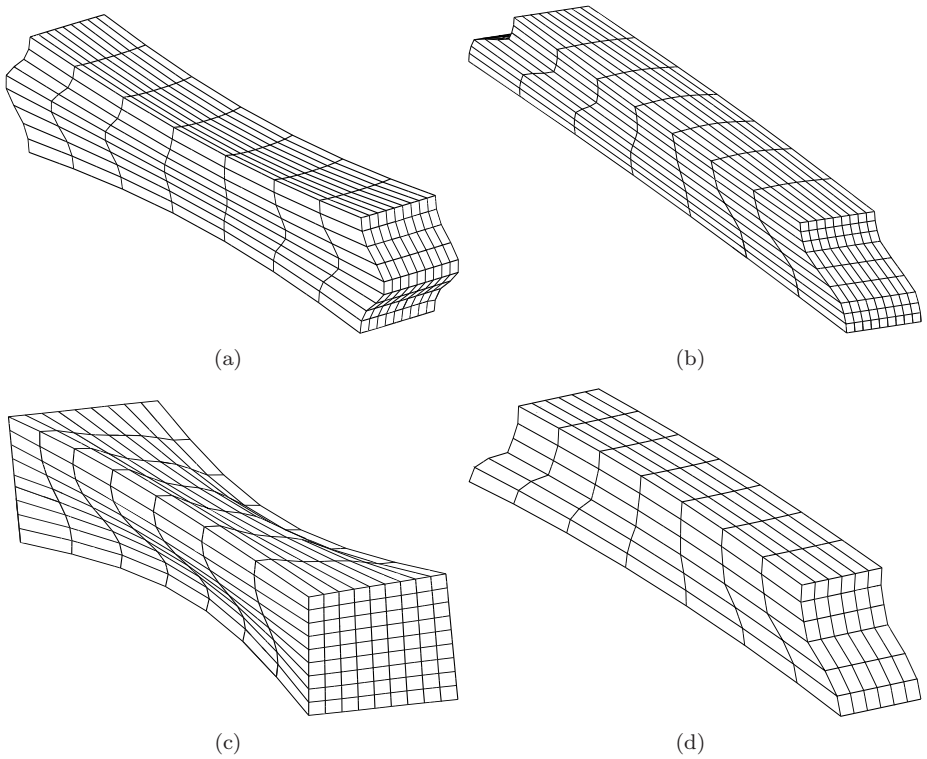

Figure 4: Modal shapes of laminated beams. (a): Axial mode; (b): Mode V of Tab.3; (c): Mode IV of Tab.4 and Mode V of Tab.5; (d): Mode IV of Tab.5.

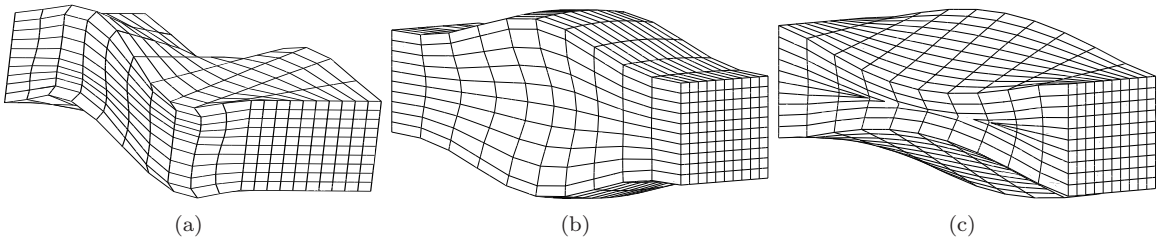

Figure 5: Modal shapes of sandwich beam. (a): Mode VI; (b): Mode VII; (c):Mode VIII.

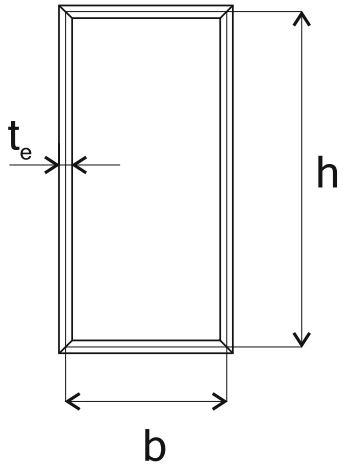

Figure 6: Sketch of the thin-walled box beam.

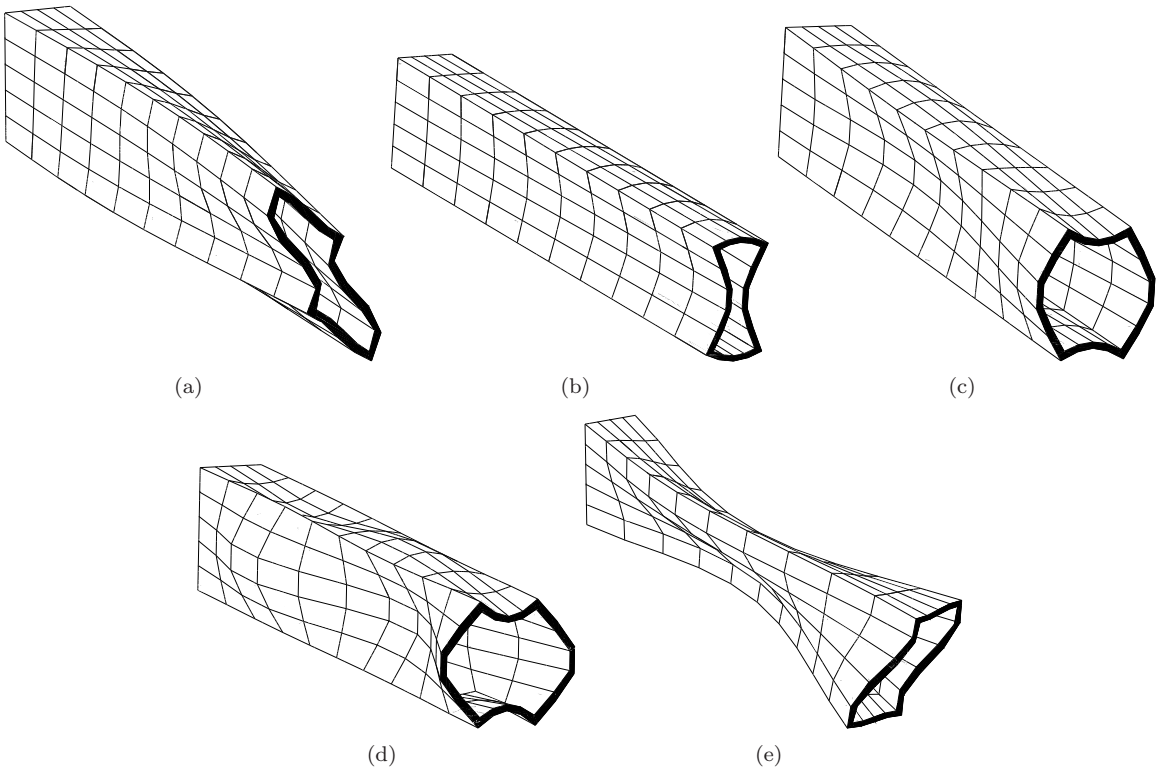

Figure 7: Shell-like modes of thin-walled box for the case $(0^0/0^0/0^0/0^0)$. (a): Mode V; (b): Mode VI; (c): Mode VII; (d): Mode VIII; (e): Mode IX